AJO-DO

Application of a new viscoelastic finite element method model and analysis of miniscrew-supported hybrid hyrax treatment

Björn Ludwig,[a] Sebastian Baumgaertel,[b] Berna Zorkun,[c] Lars Bonitz,[d] Bettina Glasl,[a] Benedict Wilmes,[e] and Jörg Lisson[f]

Traben-Trarbach, Homburg/Saar, Witten, and Düsseldorf, Germany, Cleveland, Ohio, and Sivas, Turkey

Introduction: In this study, we aimed to assess the ability of a new viscoelastic finite element method model to accurately simulate rapid palatal expansion with a miniscrew-supported hybrid hyrax appliance. **Methods:** A female patient received 3-dimensional craniofacial imaging with computed tomography at 2 times: before expansion and immediately after expansion, with the latter serving as a reference model for the analysis. A novel approach was applied to the finite element method model to improve simulation of the viscoelastic properties of osseous tissue. **Results:** The resulting finite element method model was a suitable approximation of the clinical situation and adequately simulated the forced expansion of the midpalatal suture. Specifically, it demonstrated that the hybrid hyrax appliance delivered a force via the 2 mini-implants at the center of resistance of the nasomaxillary complex. **Conclusions:** The newly developed model provided a suitable simulation of the clinical effects of the hybrid hyrax appliance, which proved to be a suitable device for rapid palatal expansion. (Am J Orthod Dentofacial Orthop 2013;143:426-35)

Initial studies with finite element method (FEM) analysis in the dental field were conducted in the 1970s.[1-7] At that time, the limited technology only allowed the use of simple models that were tailored to a specific problem. However, a decade later, Tanne et al[8] published an article and used a more complex model to simulate the effects of maxillary protraction on the midface.

[a]Private practice, Traben-Trarbach, Germany; adjunct professor, Department of Orthodontics, University of Homburg/Saar, Homburg/Saar, Germany.
[b]Associate clinical professor, Department of Orthodontics, School of Dental Medicine, Case Western Reserve University, Cleveland, Ohio.
[c]Instructor, Department of Orthodontics, Faculty of Dentistry, Cumhuriyet University, Sivas, Turkey.
[d]Department of Cranial and Maxillofacial Surgery, University Witten/Herdecke, Witten, Germany.
[e]Associate professor, Department of Orthodontics, University of Düsseldorf, Düsseldorf, Germany.
[f]Chairman, Department of Orthodontics, University of Homburg/Saar, Homburg/Saar, Germany.
Drs. Ludwig and Baumgaertel share the first author position on this paper.
The authors report no commercial, proprietary, or financial interest in the products or companies described in this article.
Reprint requests to: Sebastian Baumgaertel, Case Western Reserve University, School of Dental Medicine, Department of Orthodontics, 10900 Euclid Ave, Cleveland, OH 44106; e-mail, sxb155@case.edu.
Submitted, February 2012; revised and accepted, July 2012.
0889-5406/$36.00

http://dx.doi.org/10.1016/j.ajodo.2012.07.019

A different orthopedic measure that also affects the midface, among other areas, is rapid palatal expansion, which was initially described by Angle.[9] Further developments by Haas[10,11] and Biederman[12] established it as a well-accepted technique for the treatment of maxillary transverse deficiencies. With favorable anatomic circumstances, the traditional tooth-borne rapid palatal expander has been shown to effectively increase the maxillary transverse dimension, albeit causing considerable side effects in terms of buccal tipping of the anchorage teeth and associated fenestrations of the buccal cortical plate, root resorption, and gingival recessions.[13,14]

Rapid maxillary expansion is a rather complex treatment that was shown to have effects on the maxilla in all 3 dimensions. Traditionally, it is carried out by using a tooth-borne appliance with a center jackscrew that translates 2 equal and opposite, but collinear, forces onto the maxillary halves, attempting to spread them apart. Early experiments on dry skulls suggested that, in the coronal plane, this results in lateral rotations of both maxillary halves, with the center of resistance slightly above the piriform aperture at the frontomaxillary suture.[15] In the axial plane, the center of rotation appears to lie in the posterior maxillary suture at the level of the third molars. Lastly, sufficient evidence suggests a mild downward movement of the maxillary complex when rapid palatal expansion is applied.[16]

Fig 1. Occlusal view of the hybrid rapid palatal expander after successful expansion.

To better understand the treatment effects of rapid palatal expansion, this common treatment method has been the focus of many FEM studies in recent years.[8,17-22] The goal of our study was to test the ability of a newly developed viscoelastic FEM model to accurately simulate the treatment effects of the partially bone-borne hybrid hyrax appliance.

MATERIAL AND METHODS

This study was conducted by using existing image data of a 16-year-old female orthodontic patient who was treated for maxillary transverse deficiency with a hybrid hyrax appliance (SnapLock Expander; Forestadent, Pforzheim, Germany); it is a modified expansion appliance that is attached to the maxillary first molars and anteriorly supported by 2 orthodontic mini-implants (Fig 1).[23] This design was proposed by Wilmes et al,[24] Wilmes and Drescher,[25] and Wilmes et al[26] as the "hybrid hyrax." The 2 mini-implants (Ortho Easy; Forestadent) were 8 mm in length and 1.8 mm in diameter, and were inserted in the anterior palate, 2 mm to the paramedian aspect of the midpalatal suture. This implant location was chosen because previous studies suggested that the center of resistance of the nasomaxillary complex is located in the premolar region.[20,27] Coincidentally, this also appears to be the most ideal location for palatal miniscrew insertion from an anatomic perspective.[28,29]

For the construction of the 3-dimensional model, the patient's head was imaged by using low-dose dental computed tomography (Brilliance 16; Siemens, Munich, Germany), with a horizontal slice thickness of 0.4 mm and a vertical slice thickness of 0.8 mm, at 2 times: T1, immediately before expansion; and T2, immediately after expansion.

The image data were saved as a digital imaging and communications in medicine (DICOM) file and later converted to a stereolithography file by using OsiriX software (Pixmeo, Geneva, Switzerland). The resulting 3-dimensional images were so precise that individual sutures could be readily identified, and the skeletal treatment effect became visually apparent in terms of sutural widening (Fig 2). The 3-dimensional stereolithographic images at T1 and T2 were used for superimposition at the anterior cranial base to assess both dental and skeletal treatment effects. The changes were highlighted by using Qualify software (Geomagic, Stuttgart, Germany) (Figs 3 and 4). The T2 image serves as a reference for the simulation. By superimposing the simulated model and the actual postexpansion image, the accuracy of the simulation could be assessed. Only a high level of congruency between both would indicate an accurate simulation. To allow accurate metric comparison of the actual and the simulated treatment results, we defined different points in all 3 planes of space (Fig 5).

The first step in creating the FEM model is to generate a 3-dimensional geometric model of the skull and the dentition. This was accomplished by segmenting the computed tomography data and then converting it into stereolithographic form by using Mimics software (version 14; Materialise, Leuven, Belgium). The stereolithographic format shows a surface view of the segmented structures and serves as scaffolding for the FEM mesh. The segmenting is illustrated in Figure 6.

Subsequently, the stereolithographic model was imported into the software (ICEM 13.1; ANSYS, Canonsburg, Pa), which was used to create the appliance model. The expander and the miniscrews were modeled as computer-aided design geometry and positioned according to the situation in the live patient by using the computed tomography images as positioning aids.

The model of the expansion device was created according to the actual appliance, consisting of 2 guiding cylinders, 2 sliders, and the expander rods (Fig 7). The material properties were entered into the model according to the information provided by the manufacturer (Table 1). The relationship between the guiding cylinders and the sliders was defined based on the real function that the former will slide along the latter when experiencing a boundary condition (eg, a force or expansion/displacement). This boundary condition was applied in the model to the internal end face of the sliders according to the red arrows in Figure 7. The direction was always parallel to the guiding cylinders.

The mesh was created on the combined geometric model consisting of both stereolithographic and

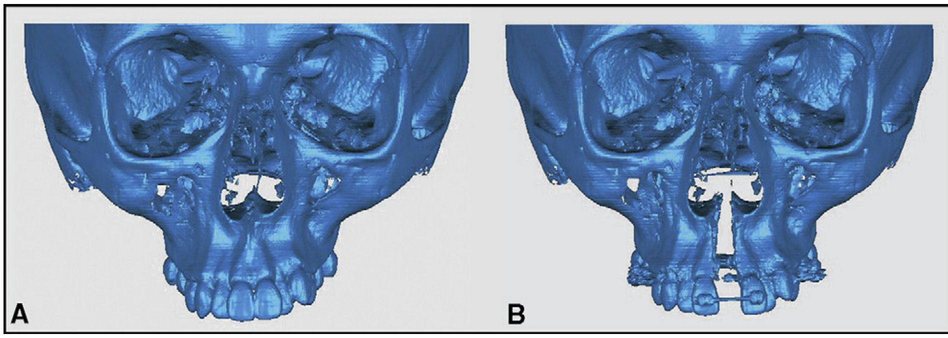

Fig 2. Stereolithographic file based on the computed tomography scans of the 16-year-old patient: **A,** preexpansion and **B,** postexpansion.

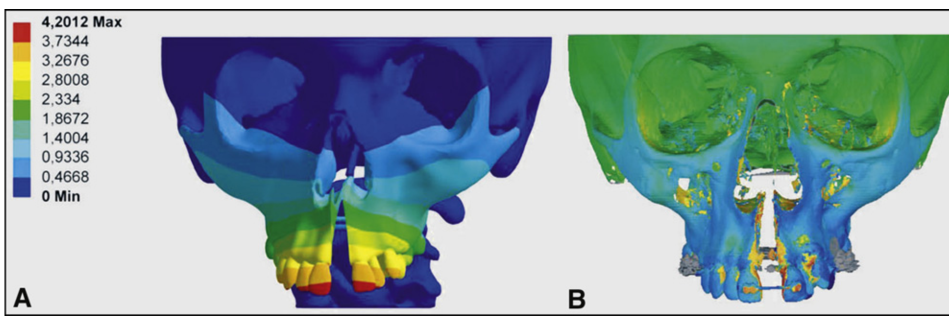

Fig 3. Frontal views: **A,** FEM simulation result with only the LeFort I level affected; **B,** superimposition with the real situation at T2 shows a nearly identical result.

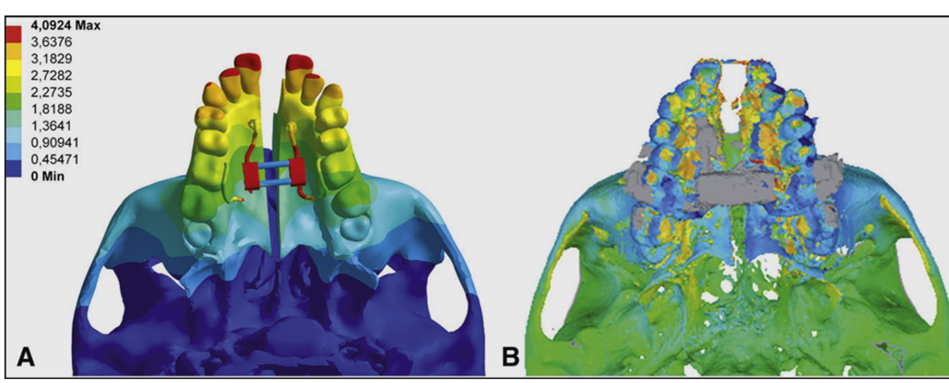

Fig 4. **A,** Occlusal view of the FEM simulation; **B,** the superimposed real T2 situation. As with the real situation, the FEM simulation changes occurred in the sutures and are therefore realistic.

computer-aided design data with the same software. Figure 8 illustrates the FEM mesh consisting of individual teeth, skull, miniscrews, expander, and expander rods, which were attached to the miniscrews at 1 end and the first molars at the other end. For reduction of complexity, the midpalatal suture was modeled without interdigitation. This should not affect the accuracy of the model because other studies clearly have shown that it is not the main source of resistance.[7,22]

Tetrahedral elements with central nodes were used for mesh generation. The resulting volumetric model consisted of 895493 volumetric elements and 202400 nodes. This level of complexity compares favorably with other studies in the current literature. Lee

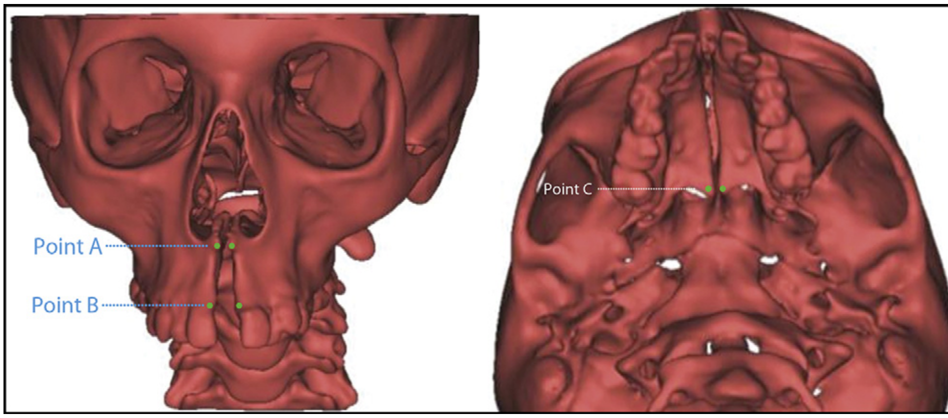

Fig 5. Location of the 3 measurement points (A, B, and C) for metric comparisons of the different simulations and the actual results.

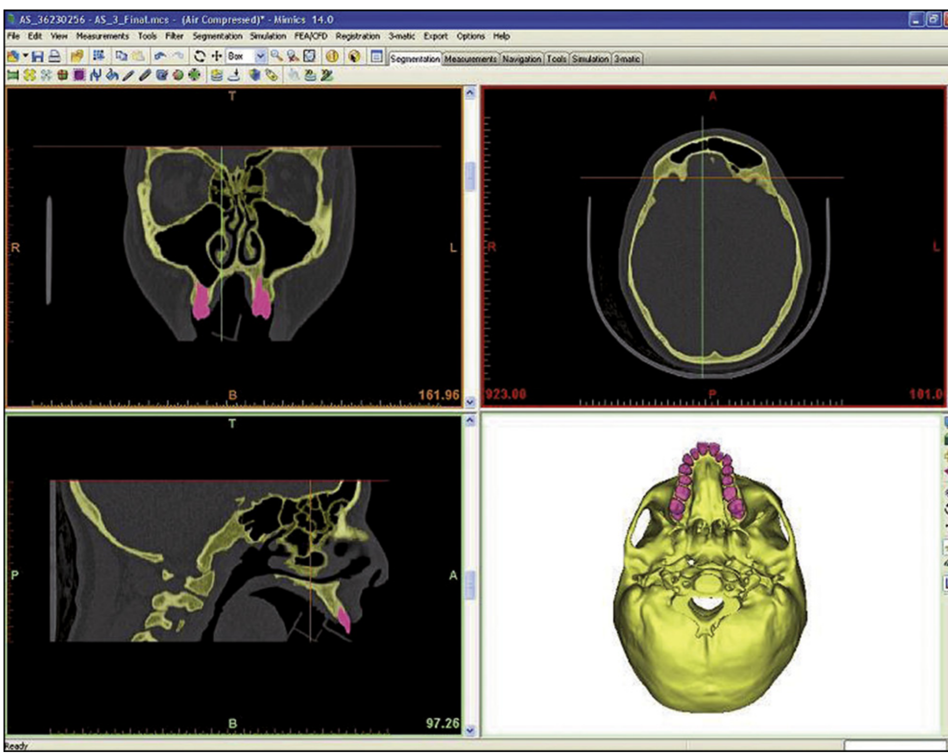

Fig 6. Segmentation of the skull and the teeth with the Mimics software.

et al,[20] for example, used 419000 elements and 100679 nodes; Jafari et al[22] used only 6951 elements and 7357 nodes.

To be able to more closely compare our setup with other studies in the literature, 2 simulations were conducted. The first (preliminary) simulation used material properties and boundary conditions commonly applied in previous studies, and the second simulation used the new, more detailed viscoelastic FEM model. Both simulations were compared with the actual treatment outcome to assess which approach more accurately simulated the actual treatment. The simulated stresses in all models for all components were von Mises stresses.

The preliminary simulation was the "conventional model." Thus far, all studies assumed linear mechanical

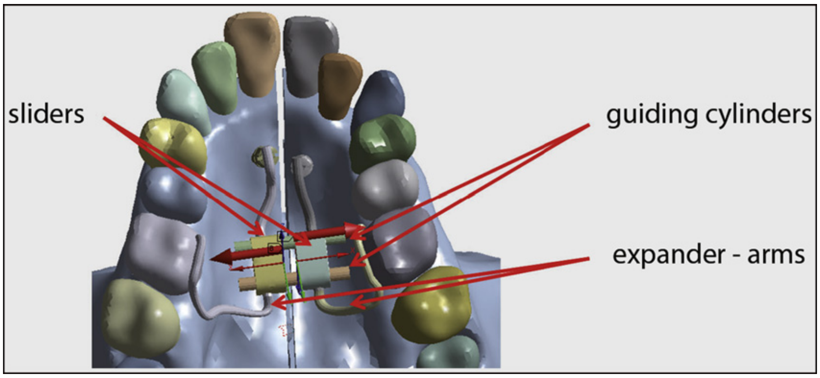

Fig 7. Expander model consisting of sliders, guiding cylinders, and expander arms.

Table I. Material properties of the expander

	Young's modulus	*Poisson's ratio*
Expander (stainless steel)	210000 MPa	0.3
Miniscrews (titanium)	110000 MPa	0.3

properties of all materials (including bone) in the FEM model.[8,17,18,21,23] All previous investigations used a Poisson's ratio of 0.3 and a Young's modulus suggested by Tanne et al[8] (Table II).

Most authors loaded the anchorage teeth with 1 constant force.[20] Alternatively, Holberg et al[18] suggested an activation of 2.5 mm per side.

For maximum comparability, the preliminary model was also built according to the method of Tanne et al,[8] and both loading scenarios described above were investigated: in the first model (model A), a constant force of 500 N was applied at the first molar and the microscrew level, and in the second model (model B), a 3.9-mm activation per side was assumed according to the clinical scenario (Fig 9).

The palatal deformation resulting from the activation was measured at 3 points (Figs 10 and 11; points A, B, and C). The results of both models were then compared with the actual measurements on the computed tomography images at T2 (Table III).

Despite an unrealistically high force application of 1000 N on either side, model A delivered deformations that were less than the actual deformations in the patient. The most likely cause for the lack of deformation was the material properties selected for the bone. If the boundary condition is based on force, increased material stiffness will lead to decreased deformation. Additionally, sutures should be considered, since they represent weak spots on the skull. The resulting V-shaped opening of the suture also appears to be different from the actual conformation.

The absolute values in model B approximated much more closely the real patient situation on the computed tomography scan. However, the deformation did not behave according to the clinical observations, since the suture opened in a more parallel fashion. Another critical aspect was the reactive forces at the anchor sites (miniscrews and first molars) in model B: with approximately 4000 N, they exceeded the maximum physiologic load by far.

In the viscoelastic FEM model, the findings from the preliminary simulations clearly showed that the linear material properties of bone and either the force-based or the expansion-based activation at the molars and the miniscrews did not reflect the real situation. The observed inaccuracies can be attributed to 2 major points.

1. The correct load transmission by the expansion appliance: if the load was generated by force or displacement, as was the case in the preliminary studies, the mechanical system was not reproduced accurately. In reality, the force was transmitted to the teeth and the miniscrews through the expansion mechanism.
2. Additionally, the load was applied to the palate incrementally; this allowed the bone to respond to the individual expansion steps. This means that the bone "relaxed" after every expansion step, reducing the osseous resistance between every activation.

To better reflect reality, the viscoelastic model was introduced; it accounted for the 2 aforementioned sources of inaccuracy.

The load transmission, discussed in point 1 above, was modeled more accurately by integrating the actual expansion protocol into the simulation. The patient had an 8-mm expansion screw, which she activated 3

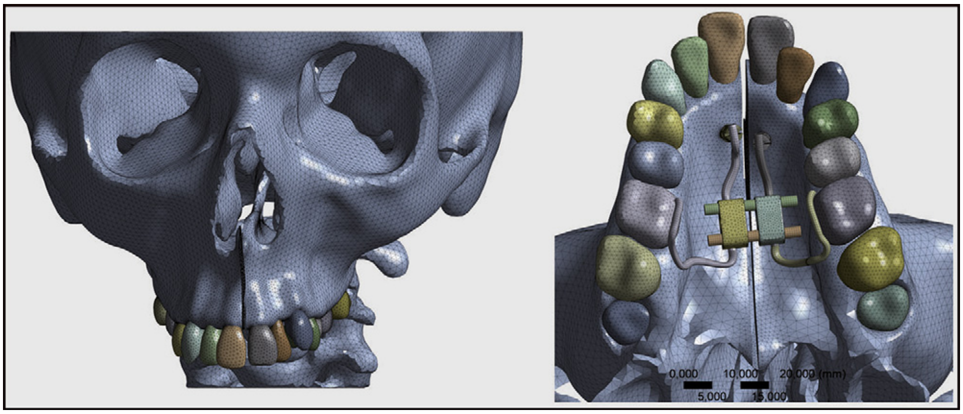

Fig 8. Final FEM model for the simulation of rapid palatal expansion treatment with the hybrid rapid palatal expander.

Table II. Material properties according to Tanne et al[8] (Young's modulus)

	Young's modulus	*Poisson's ratio*
Teeth	20000 MPa	0.3
Cortical bone	13700 MPa	0.3
Cancellous bone	7900 MPa	0.3

times a day for 13 days (1 activation, + 0.1 mm per side), resulting in 7.8 mm of total expansion (3.9 mm per side). Therefore, this FEM model applied the 3.9 mm of expansion to each side incrementally and maintained the expansion constantly for a set period of time, allowing the bone to "relax" between activations. Preliminary data analysis showed that, when the viscoelastic model was used, an activation should be performed over a 10-second period with a rest period between activations of 500 seconds to obtain realistic results.

We closely considered the relaxation behavior of the bone, discussed in point 2 above, by application of the viscoelastic model in the sense that the resistance and stresses in the bone could dissipate after an activation, allowing subsequent force application at a lower load level.

The material parameters applied in this model used the elastic properties listed in the preliminary studies and supplemented them with the viscous properties identified here.

RESULTS

When comparing the metric results at the measurement points A, B, and C (Figs 10 and 11) of the computed tomography scan at T2 (actual treatment result) and the simulated result of the viscoelastic FEM model, it became apparent that the new model can approximate the actual treatment result closely (Table IV). Superimposition of the T2 scan volume and the FEM simulation (Fig 12) resulted in high congruency (Figs 3, 4, and 12).

The results from both treatment and FEM simulations showed that the posterior skull and the anterior skull above the LeFort I plane remained unaltered. Expansion took place in the midface along the sutures. Additionally, a slight anterior and downward movement could be observed. Also with this expansion appliance, the midpalatal suture opened in a pyramid geometry, with the apex pointing cranially and posteriorly, as suggested by other authors.[30]

Figure 13 shows the stress and strain distributions in the bone. The greatest stress occurred along the sutures, especially in the area of the infrazygomatic crest. In addition, the sutures of the orbit and the posterior zygoma experienced considerable stresses. As reported previously, the entire pterygomaxillary complex showed increased stress.[17] What has not been reported to date is the enormous stress around the miniscrews, which are positioned close to the center of resistance of the nasomaxillary complex. However, due to the incorporation of endossous implants into the expansion devices, which are positioned at the center of resistance of the nasomaxillary complex, the dentition is all but devoid of stresses and strains. This even applies to the molars, which serve as additional anchors for the appliance.

Even though the slider of the expander was displaced by 3.9 mm per side both in reality and in the simulation, certain structures opened only half as much. Figure 14 shows that the rather delicate arms of the expander could only partially translate the displacement at the

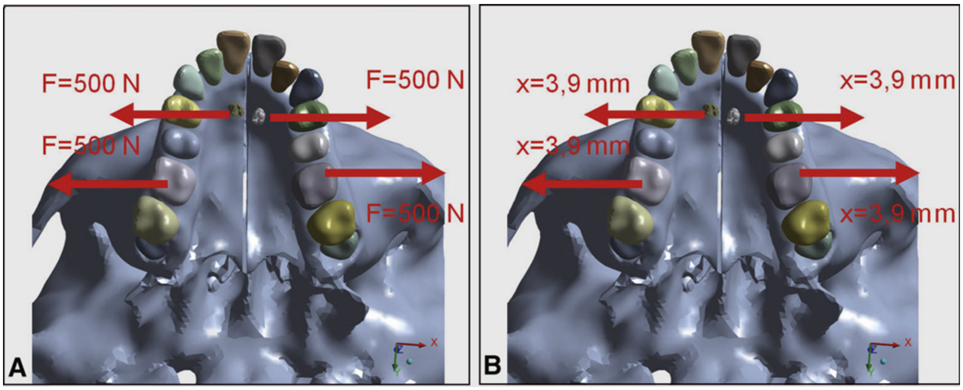

Fig 9. Investigated boundary conditions applied in the preliminary simulations: **A,** a force of 500 N was applied at the molars and the miniscrews (model A); **B,** a displacement of 3.9 mm was applied at the miniscrews and the first molars (model B).

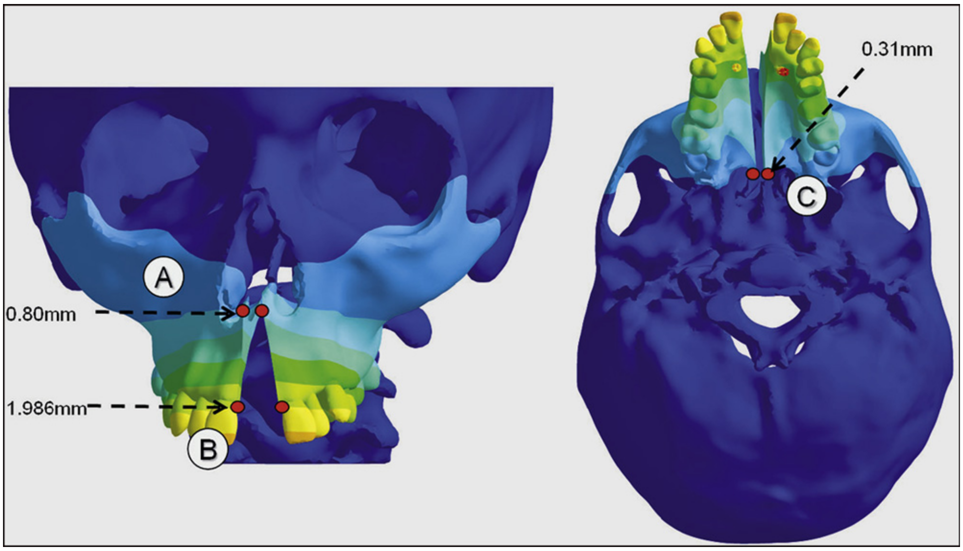

Fig 10. FEM simulation results for model A: the opening of the palate is too small compared with the clinical situation. Note that the deformation is expressed in terms of a color scale; the actual expansion is less than shown in the image.

sliders to the cranial structures, since they responded with considerable deformation themselves.

DISCUSSION

Previous FEM simulations addressing this topic were mostly conducted on artificial skulls or dry skulls of adults and children.[17,19-21] Unfortunately, the limitations of any FEM study depend on the precision of the original. Tanne et al,[8] for example, sliced a dry skull into 1-cm-thick slices and used photos taken of them as the basis for their FEM model. Other studies used computed tomography scans of artificial skulls with slice thicknesses of 2.5 to 5 mm so that details such as sutures were not visible per se. They needed to be treated with barium sulfate to become visible.[17,21,22] This could be successfully done on a dry skull. However, when we attempted to simulate a complex treatment protocol on the pretreatment records of a live patient, this approach was not viable.

This investigation showed that a high-resolution dental computed tomography scan can precisely reproduce all relevant cranial structures. On that basis, it seems that the traditional approach of cranial FEM models with little detail created on cadaver heads is obsolete. An additional advantage of the approach we

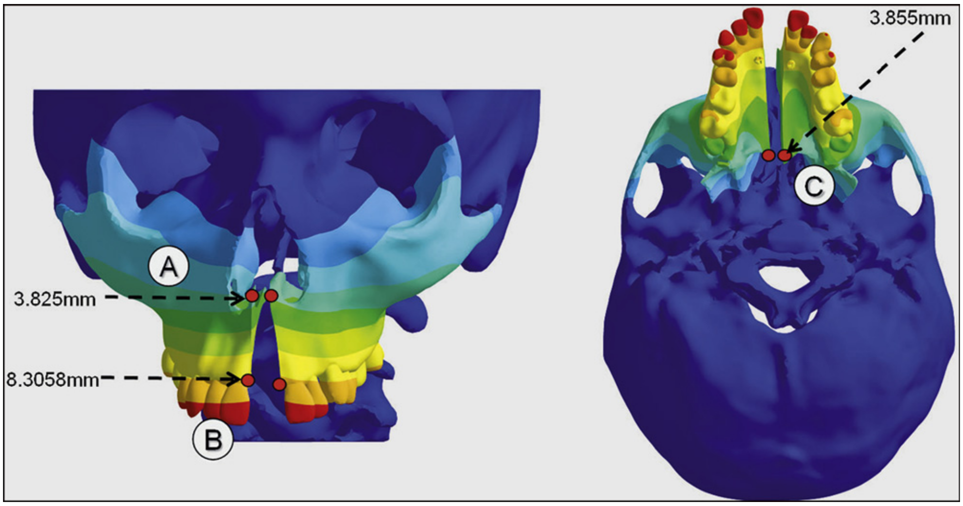

Fig 11. FEM simulation results for model B: compared with the actual situation, the opening of the palate is too great, especially at measurement point C.

Table III. Metric comparison of the preliminary (models A and B) simulation results with the actual treatment result

	A	*B*	*C*	*Ratio (B/C)*
Real patient model	6.58	3.57	1.93	1.85
Model A	1.986	0.8	0.31	2.58
Model B	8.306	3.825	3.855	0.99

Table IV. Metric comparison of the simulation results (viscoelastic model) with the actual treatment result

	A	*B*	*C*	*Ratio (B/C)*
Real patient model	6.58	3.75	1.93	1.85
Viscoelastic FEM model	6.49	3.69	1.88	1.96

chose in this study appears to be that only the direct comparison of an actual treatment result with the simulated situation will deliver a valid assessment of the level of precision achieved by the FEM model. This approach has not been described in the literature to date.

The results suggest that allowing the bone to relax in the model, as in reality, by applying viscoelastic material properties does make a difference and improves the accuracy of the simulations. Linear material properties as applied in the preliminary studies failed to accurately simulate this type of treatment. This is the first study relating to rapid palatal expansion with such a model.

The activation schedule in the model should be selected to closely resemble the actual clinical activation schedule. Simpler approaches suggested by other authors, such as applying only 1 force or a defined distance, did not reflect the real situation precisely enough and produced inferior results in the simulation.[18,20]

To further improve the precision of the simulation, we incorporated the material properties of the expander into the model. Again, this is a novel and unique approach that has not previously been described.

This study agreed with previous sources on the areas of greatest resistance and maximum stress.[20,22]

Despite the high congruency of the FEM model and the clinical reality, a limitation of this study was that the viscoelastic material properties applied here were not based on actual measurements. Depending on how these parameters are selected, simulation results can vary, especially with regard to the reactive forces at the expansion appliance. It would therefore be desirable to further improve the model by conducting more studies with additional measurements.

CONCLUSIONS

By applying viscoelastic material properties to the bone, the newly proposed model gave a realistic

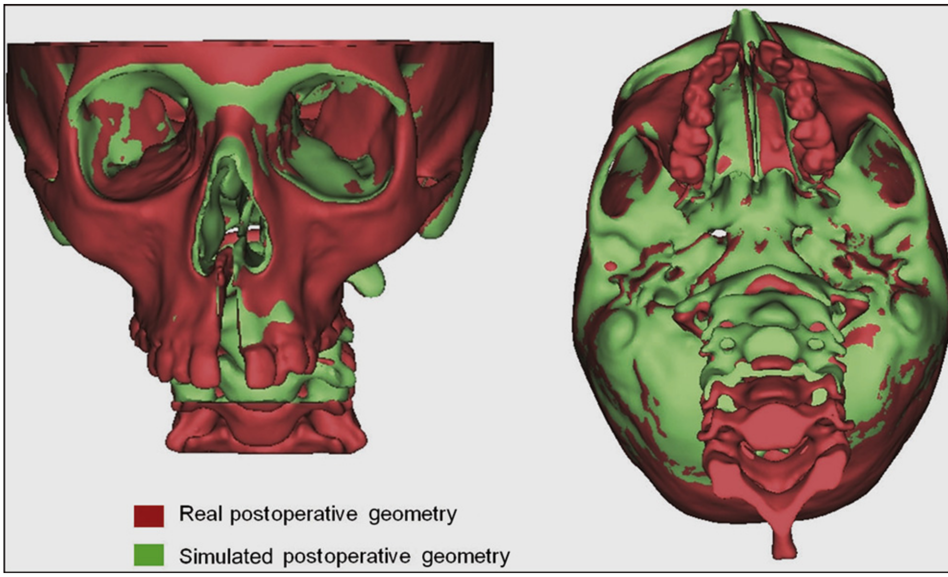

Fig 12. Comparison of the actual T2 geometry with the simulated T2 geometry from the viscoelastic model.

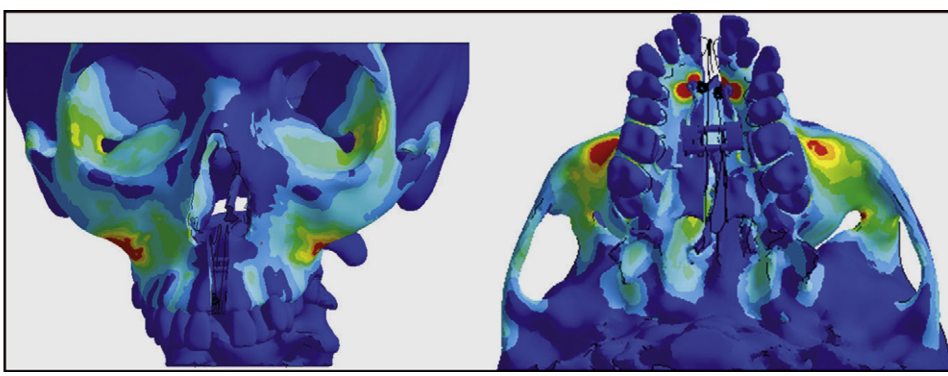

Fig 13. FEM simulations show the stresses around the sutures of the LeFort I plane.

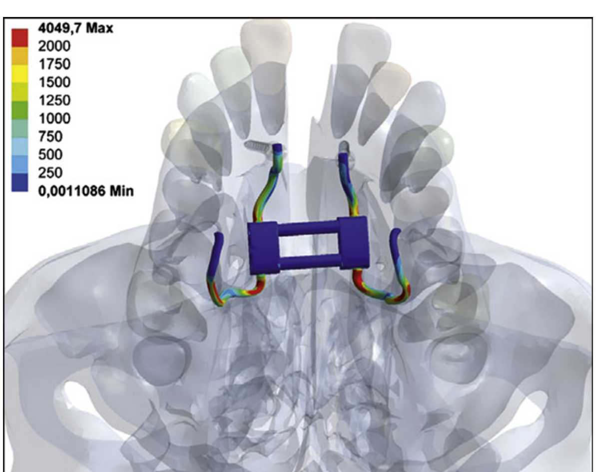

Fig 14. Deformation of the expander.

simulation of rapid palatal expansion treatment, even in complex situations. Additionally, the simulation suggested that the hybrid hyrax appliance is a biomechanically effective method for palatal expansion that prevented many of the side effects associated with the traditional tooth-borne rapid palatal expansion appliance.

We thank Christoph Müller, our engineer.

REFERENCES

1. Farah JW, Craig RG. Finite element stress analysis of a restored axisymmetric first molar. J Dent Res 1974;53:859-66.
2. Farah JW, Craig RG, Sikarskie DL. Photoelastic and finite element stress analysis of a restored axisymmetric first molar. J Biomech 1973;6:511-20.
3. Hood JA, Farah JW, Craig RG. Modification of stresses in alveolar bone induced by a tilted molar. J Prosthet Dent 1975;34:415-21.

4. Miyawaka O. Mechanical studies on the dental bridges by the finite element method (3). Behavior of a posterior bridge model under various loads (author's translation). Shika Rikogaku Zasshi 1976; 17:287-96.
5. Miyawaka O. Mechanical studies on the dental bridges by the finite element method (2). An idealized symmetrical bridge with a vertical load at the center of pontic (author's translation). Shika Rikogaku Zasshi 1976;17:278-86.
6. Miyawaka O. Mechanical studies on the dental bridges by the finite element method. (1) An abutment tooth model (author's translation). Shika Rikogaku Zasshi 1976;17:269-77.
7. Selna LG, Shillingburg HT Jr, Jerr PA. Finite element analysis of dental structures—axisymmetric and plane stress idealizations. J Biomed Mater Res 1975;9:237-52.
8. Tanne K, Hiraga J, Kakiuchi K, Yamagata Y, Sakuda M. Biomechanical effect of anteriorly directed extraoral forces on the craniofacial complex: a study using the finite element method. Am J Orthod Dentofacial Orthop 1989;95:200-7.
9. Angle EH. Malocclusion of the teeth. 7th ed. Philadelphia: S. S. White Manufacturing; 1907.
10. Haas AJ. Long-term posttreamtent evaluation of rapid palatal expansion. Angle Orthod 1980;50:189-217.
11. Haas AJ. Rapid palatal expansion: a recommended prerequisite to Class III treatment. Trans Eur Orthod Soc 1973;311-8.
12. Biederman W. Rapid correction of Class 3 malocclusion by midpalatal expansion. Am J Orthod 1973;63:47-55.
13. Landes C, Seitz O, Ludwig B, Sader R, Klein C. First experiences with a new palatal maxillary widening device (MWD) [abstract]. J Craniomaxillofac Surg 2006;34:155.
14. Landes CA, Laudermann K, Petruchin O, Mack MG, Kopp S, Ludwig B, et al. Comparison of bipartite versus tripartite osteotomy for maxillary transversal expansion using 3-dimensional preoperative and postexpansion computed tomography data. J Oral Maxillofac Surg 2009;67:2287-301.
15. Braun S, Bottrel JA, Lee KG, Lunazzi JJ, Legan HL. The biomechanics of maxillary sutural expansion. Am J Orthod Dentofacial Orthop 2000;118:257-61.
16. Majourau A, Nanda R. Biomechanical basis of vertical dimension control during rapid palatal expansion therapy. Am J Orthod Dentofacial Orthop 1994;106:322-8.
17. Gautam P, Valiathan A, Adhikari R. Stress and displacement patterns in the craniofacial skeleton with rapid maxillary expansion: a finite element method study. Am J Orthod Dentofacial Orthop 2007;132:5.e1-11.
18. Holberg C, Steinhauser S, Rudzki I. Surgically assisted rapid maxillary expansion: midfacial and cranial stress distribution. Am J Orthod Dentofacial Orthop 2007;132:776-82.
19. Holberg C, Steinhauser S, Rudzki-Janson I. Rapid maxillary expansion in adults: cranial stress reduction depending on the extent of surgery. Eur J Orthod 2007;29:31-6.
20. Lee H, Ting K, Nelson M, Sun N, Sung SJ. Maxillary expansion in customized finite element method models. Am J Orthod Dentofacial Orthop 2009;136:367-74.
21. Iseri H, Tekkaya AE, Oztan O, Bilgic S. Biomechanical effects of rapid maxillary expansion on the craniofacial skeleton, studied by finite element method. Eur J Orthod 1998;20: 347-56.
22. Jafari A, Shetty KS, Kumar M. Study of stress distribution and displacement of various craniofacial structures following application of transverse orthopedic forces—a three dimensional FEM study. Angle Orthod 2003;73:12-20.
23. Ludwig B, Glasl B, Bowman SJ, Drescher D, Wilmes B. Miniscrew-supported Class III treatment with the hybrid RPE advancer. J Clin Orthod 2010;44:533-9.
24. Wilmes B, Bowman JS, Baumgaertel S. Fields of application of mini-implants. In: Ludwig B, Baumgaertel S, Bowman JS, editors. Mini-implants in orthodontics—innovative anchorage concepts. London, United Kingdom: Quintessence; 2008. p. 91-122.
25. Wilmes B, Drescher D. A miniscrew system with interchangeable abutments. J Clin Orthod 2008;42:574-80.
26. Wilmes B, Nienkemper M, Drescher D. Application and effectiveness of a new mini-implant and tooth-borne rapid palatal expansion device. The hybrid-hyrax. World J Orthod 2010;11: 323-30.
27. Tanne K, Matsubara S, Sakuda M. Location of the center for resistance of the nasomaxillary complex studies in a three-dimensional finite element model. Br J Orthod 1995;22:227-32.
28. Baumgaertel S. Quantitative investigation of palatal bone depth and cortical bone thickness for mini-implant placement in adults. Am J Orthod Dentofacial Orthop 2009;136:104-8.
29. Ludwig B, Glasl B, Bowman SJ, Wilmes B, Kinzinger GS, Lisson JA. Anatomical guidelines for miniscrew insertion: palatal sites. J Clin Orthod 2011;45:433-41.
30. Garrett BJ, Caruso JM, Rungchatassaeng K, Farrage JR, Kim JS, Taylor GD. Skeletal effects to the maxilla after rapid maxillary expansion assessed with cone-beam computed tomography. Am J Orthod Dentofacial Orthop 2008;134:8-9.